

A Low-Cost Underwater Stereo-Camera System for Underwater Quantitative Imaging

Alexandra T. Runyan ^a, Breanna E. Motsenbocker ^a, Christopher N. Roman ^{a,b}, Russell
Shomberg ^a, Brennan T. Phillips ^{a,b}

^a University of Rhode Island, Department of Ocean Engineering, Narragansett, RI, USA

^b University of Rhode Island, Graduate School of Oceanography, Narragansett, RI, USA

Corresponding author email: alexarunyan@gmail.com

A Low-Cost Underwater Stereo-Camera System for Quantitative Imaging

Alexandra T. Runyan ^a, Breanna E. Motsenbocker ^a, Christopher N. Roman ^{a,b},
Russell Shomberg ^a, Brennan T. Phillips ^{a,b}

^a *University of Rhode Island, Department of Ocean Engineering, Narragansett, RI, USA*

^b *University of Rhode Island, Graduate School of Oceanography, Narragansett, RI, USA*

ABSTRACT

Structure-from-Motion (SfM) photogrammetry has become an increasingly useful tool in recent years for underwater surveys of seafloor environments. The current method involves divers placing physical ground control points (GCPs) and scale-bars on the substrate, swimming in a boustrophedon pattern over the substrate, and taking several overlapping images with high-cost digital cameras. The necessity of GCPs and divers when using a single camera greatly limits the depths in which spatially rectified SfM photogrammetric reconstructions can be created. The introduction of stereo-camera systems, when properly calibrated, can remove the need for GCPs and scaling objects, allowing autonomous and remotely operated vehicles to facilitate quantitative image surveys of benthic environments beyond diver-depths. Many ecological applications for using stereo-camera systems, including SfM and accurate measurement of mobile fauna, make the necessity of a low-cost underwater stereo imaging system crucial for efficient monitoring of marine ecosystems. This study presents the design of an underwater StereoPi, a compact and low-cost stereo imaging system designed using RaspberryPi components and encased in a stereolithography (SLA) 3D printed resin housing, as well as an open-source calibration and image processing workflow using Python 3.9 and Agisoft Metashape Professional. Underwater calibration data, including comparative hydrostatic tests, are presented to determine how hydrostatic pressures affect the system's accuracy of stereo imagery measurements and spatially rectified reconstructions in deep water. The presented system has been field tested in Bermuda using a fiber optic tethered remote system for real-time

disparity map viewing through first-person goggles to a depth of 70 meters, as well as a diver-held system in Panamá for benthic SfM photogrammetry.

1. INTRODUCTION

Structure-from-Motion (SfM) photogrammetry is a frequently used imaging tool to create 3D reconstructions from overlapping imagery. SfM has only become prevalent for surveying the underwater environment in recent years, despite being widely used for land-based 3D reconstruction (Ferrari et al. 2022). Currently, the most common form of SfM photogrammetry surveys underwater involve divers swimming in a boustrophedon pattern over the substrate, taking several overlapping images with a single digital SLR camera and placing ground control points (GCPs) and scale bars on the bottom to be captured during the survey for spatial rectification during post-processing (Fukunaga et al. 2019). This method has several limitations, including small spatial scale, limited diver bottom time, and limited depth. The necessity of GCPs, scale bars, and divers when using a single camera greatly limits the depths in which SfM photogrammetric maps can be created. While single camera SfM provides impressive 3D reconstructions, deployment differences or differences in diver image collection can lead to a wide range of measurement error which can muddle important fine scale details for underwater ecologists (Jackson et al. 2020). The introduction of stereo camera systems, when properly calibrated, can remove the need for scale bars and GCPs, thus removing the diver from the equation (Hatcher et al. 2020) when the stereo camera is attached to remotely operated vehicles (ROVs), autonomous underwater vehicles (AUVs) and even Lagrangian floats (Armstrong et al. 2019). This is possible due to the geometries of the stereo pair allowing for direct mapping of features from 2D to 3D when they appear in both images.

The ecological applications for using stereo-camera systems make the necessity of a low-cost, deep stereo system crucial for efficient monitoring of difficult to access marine ecosystems. Stereo vision can be used for SfM 3D reconstruction (Andono et al. 2012), as mentioned above, to create high resolution 3D reconstructions of benthic environments, extending beyond shallow-water coral reefs to deep-water cliffs (Van Audenhaege et al. 2021) and shoreline structures of interest (Lawrence et al. 2021). These reconstructions make it possible to quantify changes in benthic communities over time and determine, to a species level, how much benthic invertebrates have grown or eroded between reconstructions. This information is invaluable in ecosystem resource management efforts as well as restoration efforts. For example, single-camera SfM photogrammetry techniques were employed at a *Sabellaria alveolata* reef habitat at Llanddulas, Wales, UK to attain habitat-scale data and glean spatial

patterns for this reef site (Jackson-Bue et al. 2021). Because it was a single-camera system, GCPs were necessary for scaling and alignment for 3D reconstruction. Using a stereo-camera system for this survey would have removed the need to place GCPs within the survey area for scaling and image alignment, making it a useful tool for capturing fine scale information over large or difficult to access areas. However, stereo camera systems must be properly calibrated for accurate measurements, and many systems face issues with calibration stability. Often, changes in the relative orientation of stereo cameras can occur before, during, or after an underwater dive, making recalibration necessary (Harvey & Shortis 1998; Schmidt & Rhzanov 2012). Thus, the necessity for a rigid system with fixed relative camera orientations and a set focus arises.

Stereo camera systems currently being used for underwater imaging are either high-cost systems (Edwards et al. 2017)), surface towed systems (Hatcher et al. 2020), or low-cost shallow systems (Oleari et al. 2014). As part of the 100 Island Challenge, Scripps Institute of Oceanography has employed a custom stereo camera rig from two Nikon D7000 16.2-megapixel DSLR cameras in underwater housings and attached to a rigid frame for their SfM surveys (Edwards et al. 2017). At approximately \$1,000 per camera and \$4,000 per underwater housing, the total cost of this systems is about \$10,000, making it inaccessible for smaller communities hoping to conduct meaningful surveys for quantitative ecology to inform long-term monitoring and conservation efforts. A lower-cost deep system was developed for the triggered stationary imaging of mobile fauna, that consisted of two Canon PowerShot 300 HS cameras (~\$100 each) built onto a RaspberryPi board (Williams et al. 2014). While this stereo camera system seems to be the most affordable deep-sea stereo camera present in the literature, it is designed for stationary deployments using a red-light trigger to take imagery of mobile fauna. There is a significant lack in low-cost repeatable stereo camera systems for use in SfM photogrammetric reconstructions for quantitative ecology in environments outside of recreational diver limits. This paper investigates the design of Underwater StereoPi and the implementation of stereo SfM techniques to replicate the existing methods of 3D benthic reconstruction.

2. METHODS

1. Design

Electronic components of the system include a StereoPi v0.9 RaspberryPi board running on a RPi Compute Module 3 that supported two RPi v2 cameras, with center of the sensors set

6.9 cm apart (Figure 1A). Each RPi v2 cameras have a maximum still resolution of 8 Megapixels, a Sony IMX219 sensor with 3280x2464 pixels each of 1.12x1.12 μm in size. Because both cameras were supported by the StereoPi v0.9 board, image pairs are captured completely in sync in a single image. RPi v2 camera modules have a rolling shutter, which is important to consider when choosing a lighting system. Consistent lighting is more appropriate for use with the rolling shutter feature, as strobes may be too fast for proper lighting to be captured within an image. Ethernet and Bluetooth were both used for communication with the system for video and image capture adjustments and data retrieval.

The stereo camera underwater housing (Figure 1A) in this study was designed in Solidworks 2020 and printed using a Formlabs SLA 3D printer. It incorporates two DEEPI camera fixtures partially filled with epoxy and covered by a ¼ inch (6.3 mm) thick piece of glass using methods described in Phillips et al. (2019). A laser-cut 3/8" acrylic plate was used to seal the top of the housing with a polyurethane gasket. A 13-pin bulkhead wet connector supplies power and bridges a gigabit ethernet connection to the electronic system when deployed as a tethered system. A 3.67V battery fits within the housing design (Figure 1A) for diver deployments where internal power is necessary and can support the collection of 24 fps video for approximately 6 hours. Field trials were conducted in Bermuda at the Bermuda Institute of Ocean Sciences (BIOS) in May 2022, in Panamanian waters in June 2022, and in Point Judith Pond, RI, USA in October 2022.

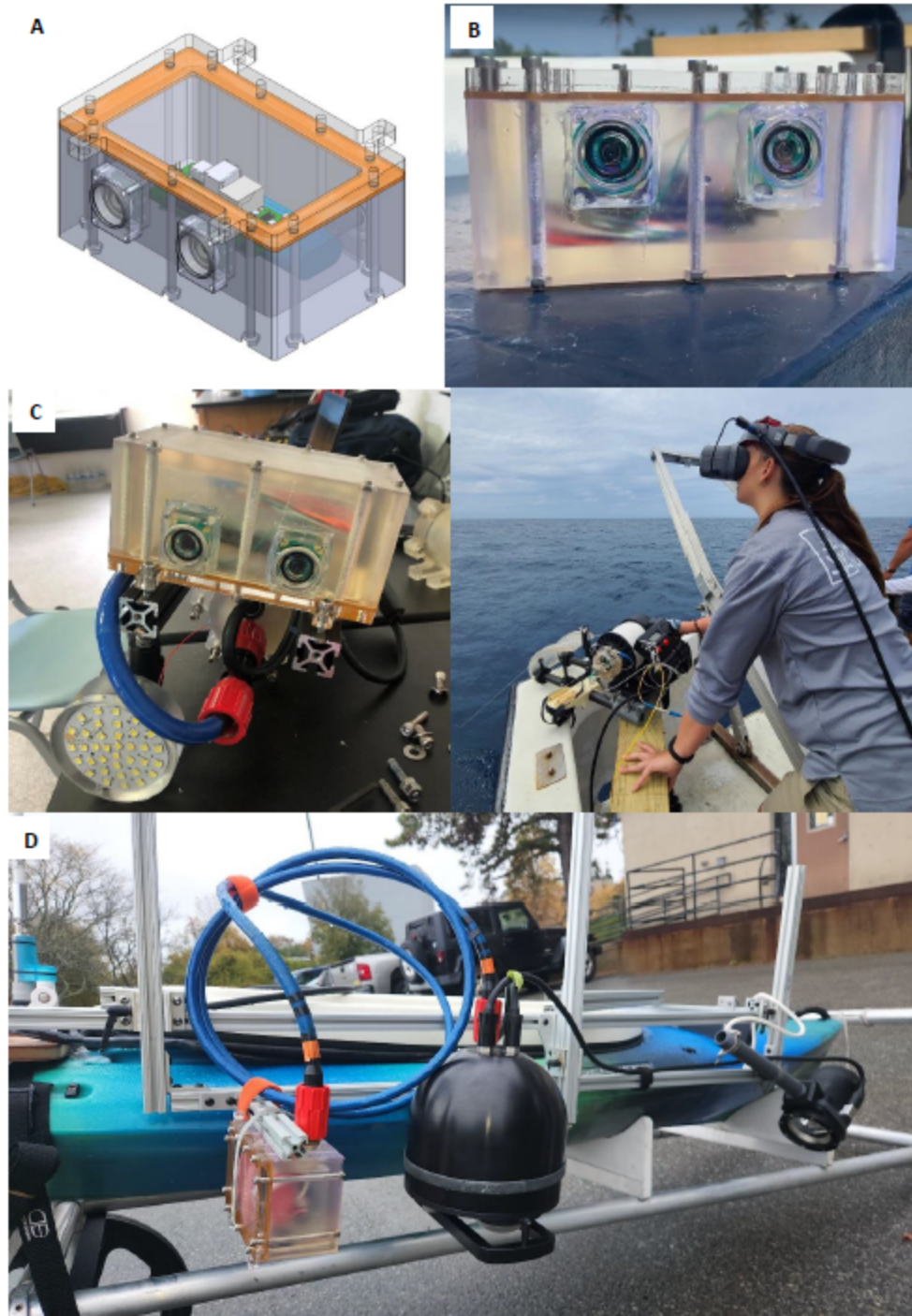
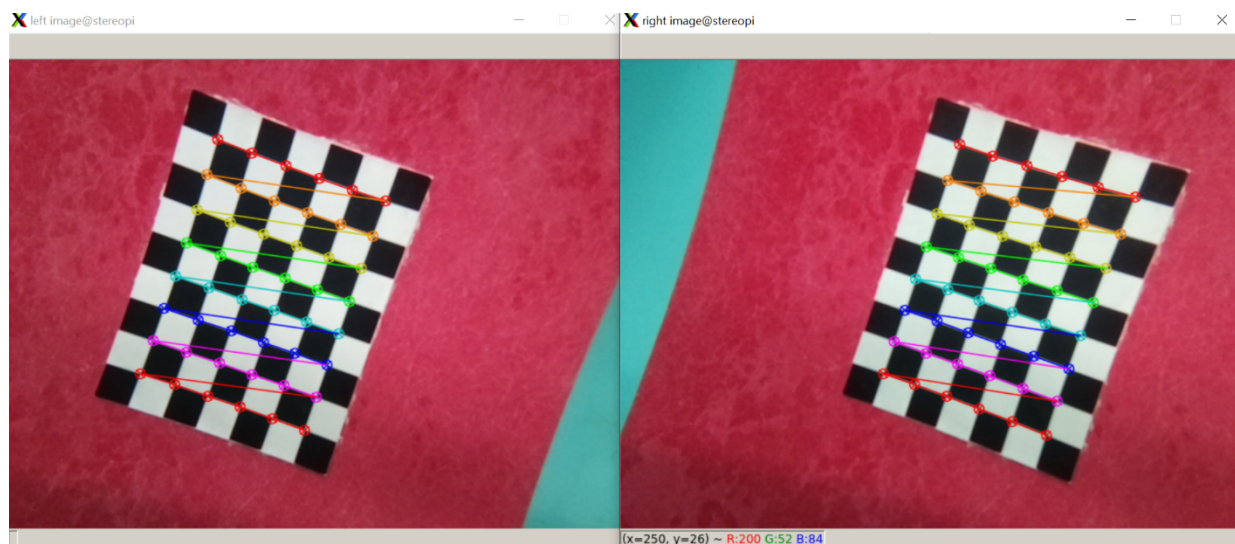


Figure 1. Underwater StereoPi housing design and configurations for three field deployment styles. a) AutoCAD model of underwater housing with battery, b) diver-held, battery-powered set up for deployment over coral reefs in Panamá, c) underwater StereoPi payload for remote tethered deployment through fiber-optic fishing line, d) set up for autonomous kayak surveys.

2. Calibration

Stereo calibration and image rectification scripts were written using Python 3.9 and OpenCV (https://github.com/atrunyan/stereopi_URI). OpenCV's calibration function is based on the algorithms created by Z. Zhang (2000) and JY. Bouguet (2004). A 9x7 checkerboard was laser cut from acrylic sign material and mounted to a bend-resistant fiberglass board for the most accurate calibration possible. Initial calibration was conducted in a large freshwater tank on University of Rhode Island's Narragansett Bay campus, collecting approximately 50 paired photos of the checkerboard at several different angles (Figure 2) (Andono et al. 2012). A 1-meter distance was used to calibrate the system at the same distance as altitude during SfM surveys.

Depth calibration trials were also conducted within a large pressure tank in the University of Rhode Island's Dynamic Photomechanics Laboratory (Shukla et al. 2018). Image sets of 5 checkerboard targets, one 9x7 and four 3x2 in the corners of the fiberglass board set 1 meter away from the camera, were taken at 10 psi intervals until 150 psi (~105-meter equivalent water depth). These calibration results were compared as a function of pressure to determine the validity of stereo rectification and measurement at depth. The images were also used to create homography transformations to visually assess whether there is a significant pixel shift of the targets between shallow and deep images.



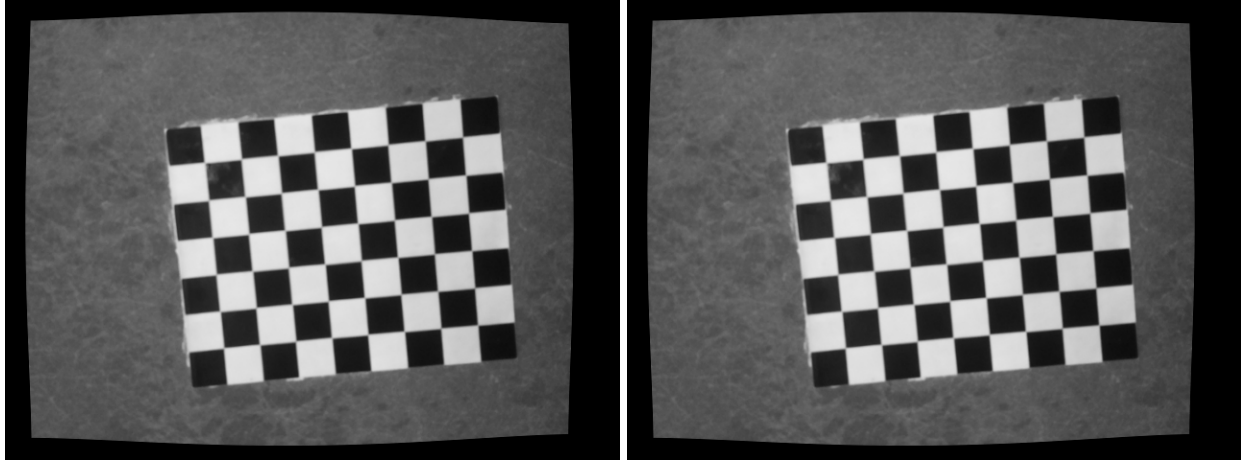


Figure 2. (Top) Examples of checkerboard photos for calibration with corner detection applied. (Bottom) Rectified images of the checkerboard after calibration, from the left and right camera, respectively.

3. Disparity Map Creation

Disparity maps were created for each deployment scheme using Python 3.9 and OpenCV. Stereo semi-global block matching was used, implementing a slightly modified version of the H. Hirschmuller (2008) algorithm where blocks are used instead of pixels, the mutual information cost function is not implemented, and pre- and post- filtering steps are included. Several parameters, including pre-filter cap, block size, minimum disparity, number of disparities, speckle range, and speckle window size, can be manipulated to change the quality of resulting disparity maps. For images collected from areas with hard bottom substrate and significant local elevation changes, pre-filter cap was set to 29 pixels, block size to 11 pixels, minimum disparity to -32 pixels, number of disparities to 160 pixels, speckle range to 16 pixels, and speckle window size to 200 pixels. For images with less local elevation changes or vegetative bottoms, parameters were kept the same except block size and speckle window size, which was set to 21 and 75 pixels respectively.

4. SfM Photogrammetric Reconstruction

For 3D reconstruction, 1 frame per second (fps) image stills were extracted from video collected during field trials to and uploaded into Agisoft Metashape Professional (Agisoft LLC., St. Petersburg, Russia) for photo alignment and rectification. Image processing workflow followed the recommended reconstruction workflow in Burns et al. 2019, with slight changes to the steps involving GCPs, as the relative position and distance of the cameras within the system

were used to calibrate and scale the model. The distance between the cameras (6.9 cm) along with intrinsic and extrinsic camera parameters were used in a simple python script to create scale bars between pairs of images to rectify the scale of the 3D reconstruction. For the most accurate reconstruction with the chosen 1280x480 total resolution for the stereo camera images, tie points were generated using the highest accuracy and generic preselection settings, as well as key point and tie point limits of 40,000 and 4,000 respectively.

3. RESULTS

1. Field Trials

A. Bermuda Fiber Optic Fishing Line (FOFL) Deployment

The stereo-camera system within its housing was connected to a battery via 13-pin wet connector and gigabit ethernet was communicated through a fiber optic microcontroller (Phillips et al. 2021). Live feed from the stereo camera was visible on a laptop as well as through first person view goggles (Figure 1). An LED light was also operated via ethernet from the laptop, to provide optimal lighting for collecting underwater footage. As the camera payload was lowered into the water, the fiber-optic reel system operator received real-time visual information from the first-person viewer goggles which allowed them to visually guide the altitude of the camera over the seafloor. Video and disparity maps were collected at approximately 70-meter water depth while the surface vessel drifted over a coral reef and the camera system was held about 1 meter from the substrate (Figure 3).

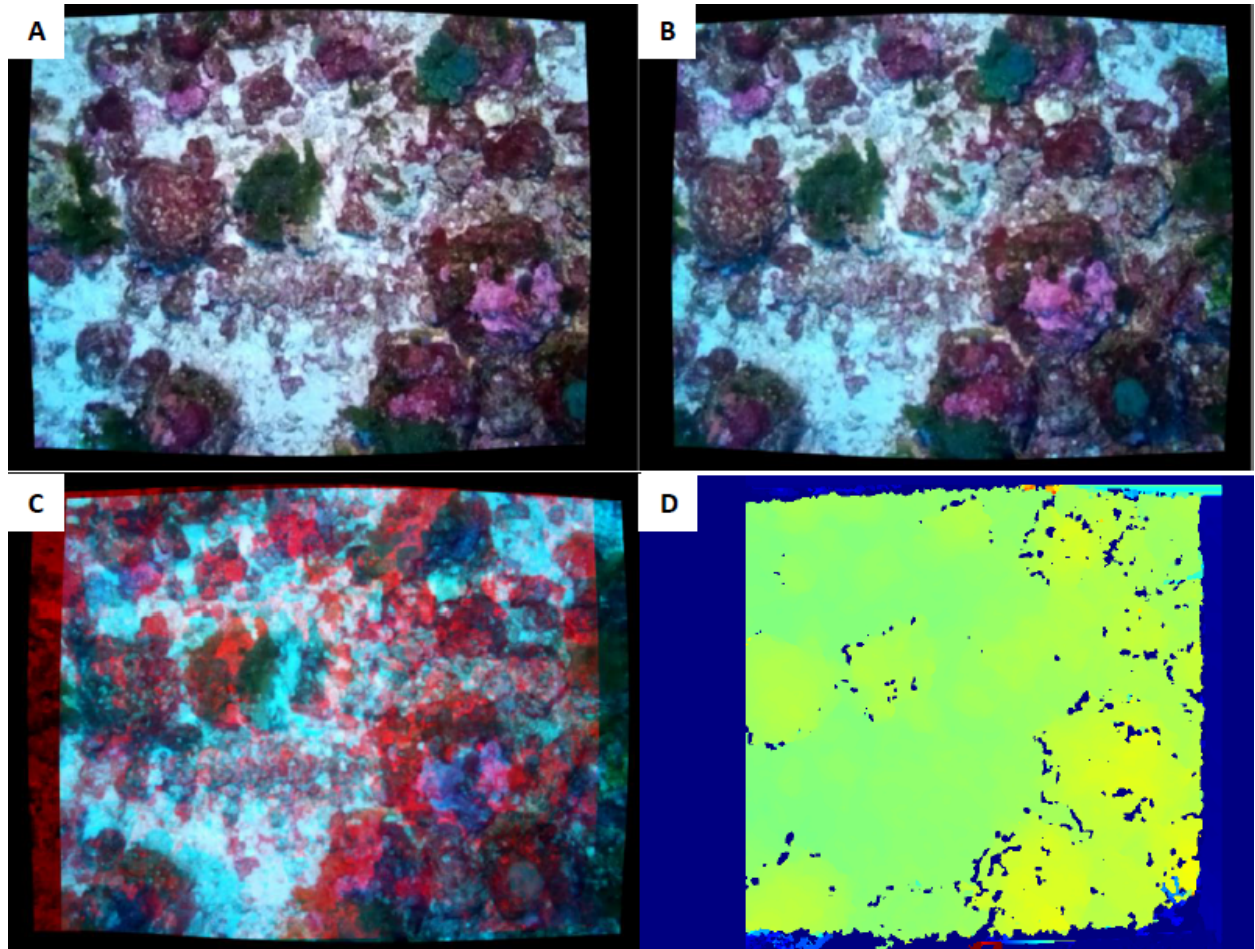


Figure 3. Images collected at 70 meter water depth off the cost of Bermuda showing a) rectified image from left camera, b) rectified image from right camera, c) image overlay of the L/R rectified images, and d) image disparity computed from calibration data where warmer colors represent higher disparity (areas closer to the cameras).

B. Panamá Diver-Held Stereo Video Collection

For diver-held video collection, the stereo camera system was rigged in its usual underwater housing with a flexible light arm attached to the acrylic top, allowing for mounting an external light source with its own power (Figure 1A, 1B). A Python script was set up to record video on boot up of the stereopi board, allowing the rig to be disconnected from an ethernet tether and run only on battery power. Video imagery was collected via diver by swimming the camera in a boustrophedon pattern 1 meter above the reef (Fukunaga et al. 2019). Divers swam slowly over the reef to ensure ~80% or greater frame overlap throughout the 24-fps video. For the purposes of assessing the effectiveness of this stereo camera system in rectifying 3D reef models, no scale bar or target was deployed on the seafloor during these surveys.

2. Calibration Tests

Initial calibration testing within URI Bay Campus' freshwater tank resulted in reprojection error of 0.1429, 0.1487, and 1.0919 pixels for the left camera, right camera, and stereo reprojection respectively. Visually, rectified images of the calibration board show distortion correction, in that the straight lines of the checkerboard are straight, and the edges of the photo show a resulting barrel effect to offset the camera distortion underwater (Figure 2). Radial distortion coefficient values from calibration sequences were negative, confirming that the cameras produce a pincushion distortion that is offset in rectification by creating a slight barrel.

Pressure calibration tests showed insignificant differences in distortion between pressures. At 150 psi, resulting reprojection error for the left camera, right camera, and stereo reprojection was computed to be 0.1697, 0.1367, and 0.8271 pixels respectively. Homography testing of the 0 psi image with a 150 psi image showed that distortion of the camera housing under pressure is negligible and does not significantly affect image alignment at depth (Figure 4). Distortion coefficients were also compared for every 10 psi between 0 psi and 150 psi calibrations. The coefficients do not seem to show a direct relationship with pressure and have very minor variations, except for the right camera at 80 psi, which shows a distinct outlier, likely a result of an air bubble or other obstruction blocking the camera's view of the calibration targets (Figure 5). Overall, distortion coefficients appear to remain within 0.2 pixels (0.1% change between surface and depth) of radial distortion and within 0.02 pixels (0.01% change between surface and depth) of tangential distortion.

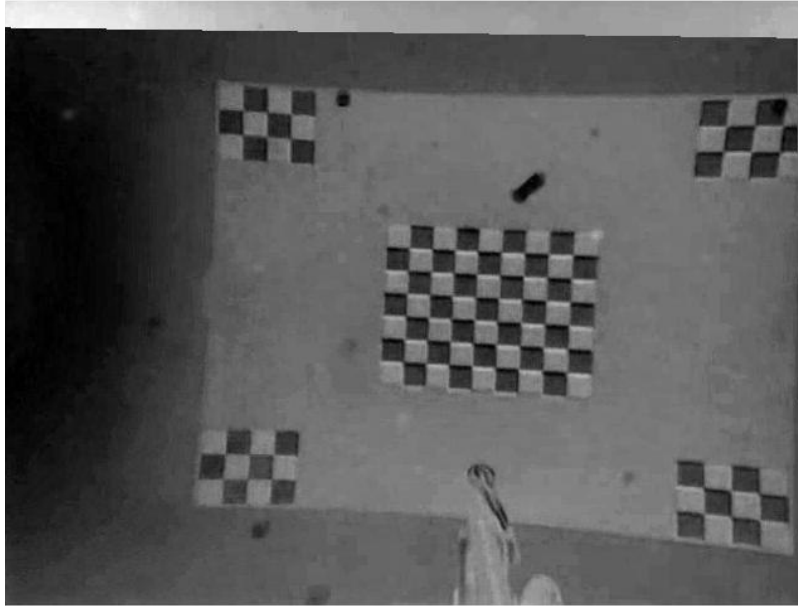


Figure 4. Homography overlay of calibration board taken at 0 psi and at 150 psi.

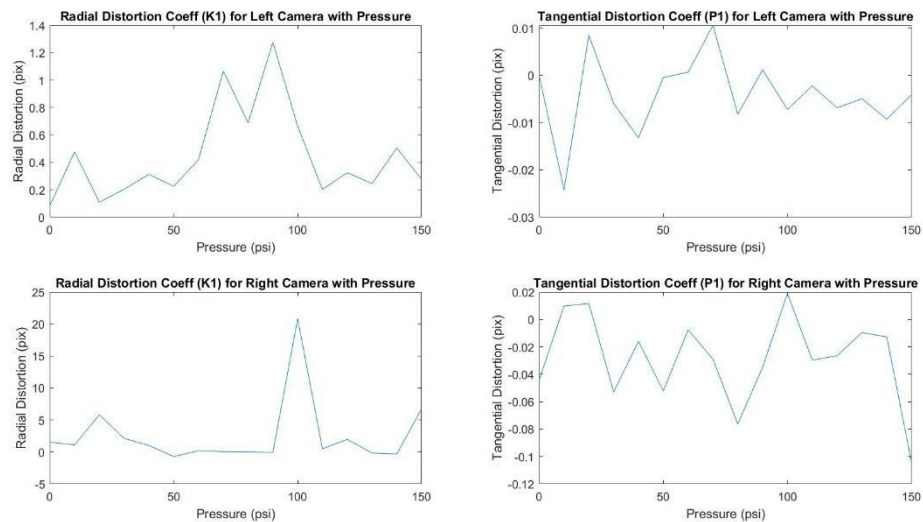


Figure 5. Plots of distortion coefficients versus pressure for left and right cameras.

3. SfM Photogrammetric Reconstructions

A small reef site, with maximum depth of 39 feet, known as Incubator Reef in Portobelo, Panamá was reconstructed using the Metashape workflow. The reconstruction resulted in 80,113 tie points, which were used to create a dense clous of 209,770 points, a 3D model mesh with 59,999 faces, and an orthomosaic of dimensions 1855x1601 pixels and a resolution of 3.53 mm/pixel (Figure 6). As is common with photomosaics, some distortion is apparent around the

edges of the model where insufficient overlap was collected. In addition, it appears that there are some features that did not quite align with the camera calibration and stick out above the model (Figure 6B).

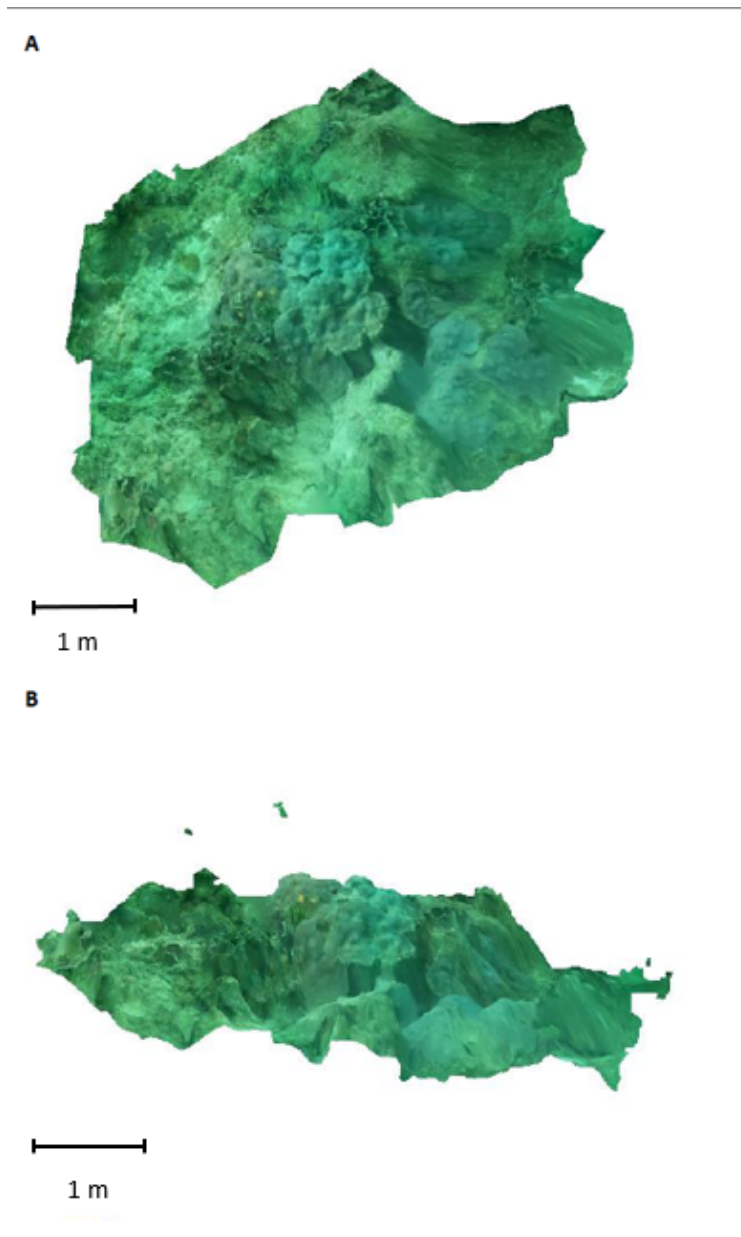


Figure 6. An orthomosaic of a small portion of Incubator Reef (max depth 39 feet), Portobelo, Panamá, featuring corals, rock, and sandy substrate. a) shows a top-down projection of the reconstruction and b) shows a side projection.

4. DISCUSSION

The design and functionality of a low-cost underwater stereo imaging system running on a Raspberry Pi Compute Module 3 and using two RPi v2 camera modules was demonstrated

during the scope of this study. While this design is not currently optimized, it was created as a prototype for practical assessment and flexibility of deployment schemes. It can be easily scaled for deeper environments by creating thicker walls or using epoxy potting methods described in Phillips et al. (2019). Using a Raspberry Pi/Linux-based framework also allows for easy customization of the camera module used and camera settings before and during deployments to suit the needs of the surveyor. At the time of its creation, the newest RPi camera module was the 8-megapixel v2, but the 12.1-megapixel v3 has since been released. The newer camera module could be used for a future iteration of Underwater StereoPi, if such a resolution was desired. Resolution can also be easily adjusted within the video capture scripts when enabling the camera module, depending on application of the resulting 3D reconstruction.

Direct syncing of the RPi v2 camera modules through the single board as well as having the cameras epoxy potted into the rigid housing makes this system more convenient than other low-cost stereo camera systems, such as GoPro stereo systems (Schmidt & Rzhano, 2012). First, syncing two GoPros together is significantly more challenging than simply attaching two RPi camera modules into the StereoPi board and can experience drift in time synchronization. Secondly, the housing used for stereo GoPro set up has a short baseline (3.5 cm; Schmidt & Rzhano, 2012) and requires the cameras to be removed to extract data from, negating the calibration as the orientation of the cameras could be slightly changed. With underwater StereoPi, cameras are on a 6.9 cm baseline, providing good geometries when taking SfM images 1 meter from the substrate, and cameras are potted within the housing, so no movement occurs before, during, or after deployment, making recalibration unnecessary. Additionally, hydrostatic calibration testing shows that distortion coefficients do not scale with increased pressure on this housing design, confirming that surface calibration is valid for data collected in deeper water, at least up to about 105 meters.

For 3D reconstructions, differing image resolutions could be tested to determine the optimal resolution for coral species identification and boundary detection with a low-cost system. With the release of the RPi v3 camera module, an additional model of underwater StereoPi could be created to mimic the high-cost camera system being deployed by the Scripps Institute of Oceanography 100 Island Challenge (Edwards et al. 2017). In addition, the stereo camera system could be outfitted to an ROV or AUV and use global positioning information from the vehicle's instrumentation to further rectify the reconstructions in a global reference

frame. Adding position information from an AUV or ROV, or even a handheld GPS system marking the start of a survey at the surface by a diver during a diver-held survey, would allow reconstructions to include valuable digital elevation models (DEMs) for accurate structural analysis of coral reef plots and ensure greater accuracy of reef models.

Another application for underwater StereoPi could be the accurate measurement of mobile fauna. Forward-facing stereo camera data in conjunction with object detection algorithms and depth measurements from calibrated stereo vision can accurately size mobile fauna, regardless of orientation to the camera systems (Dunlop et al. 2015). Many fisheries are interested in utilizing stereo cameras for counting, sizing, identifying fish species using measurements from calibrated cameras in conjunction with machine vision approaches (Ubina et al. 2022). The modularity of this underwater StereoPi system makes it simple to attach to many different deployment methods, as described in this paper, making it a valuable tool to ecologists in many different sectors of marine science. With customizability for resolution, frame rate, and other parameters, users of this system can tailor the settings to their survey needs for data collection and processing. Both capable of running tethered and on battery power, the Underwater StereoPi is useful in many survey scenarios including measurement of mobile fauna during baited remote underwater video (BRUV) surveys and 3D reconstruction of benthic environments from diver, ROV, or AUV surveys. Disparity calculations can be conducted in real-time during a live-feed deployment, to give depth feedback to an operator of an ROV. Currently, it appears that Underwater StereoPi is much lower in cost than other underwater stereo systems described in the literature (~\$500) for the use-case of SfM photogrammetry in quantitative ecology applications. This opens the opportunity for long-term monitoring efforts for communities without access to several thousand-dollar systems and research vessel accessibility.

5. CONCLUSIONS

This paper describes the design of a low-cost underwater stereo camera system with applications in quantitative ecology. It serves as a proof of concept for using Raspberry Pi-family boards and camera modules to collect imagery using known structure-from-motion methods for 3D reconstructions of benthic environments. Robust calibration of potted cameras producing sub-pixel reprojection errors within the rigid housing provides accuracy in repeated surveys at

depths exceeding 100 meters without the need for additional calibration sequences. This stereo camera was deployed as a remote-tethered system in Bermuda, on an autonomous surface vehicle, and as a diver-held system in Panamá. 3D-reconstructions of coral reefs were produced with low reprojection error values and comparable resolution to other higher-cost system. After testing this system with three different deployment methods, the ideal deployment that should be targeted would be AUV or ROV SfM surveys over coral reef environments. Using the camera calibration information in conjunction with positioning data from an underwater vehicle will create optimized 3D reconstructions and allow for gathering information over greater areas.

Acknowledgements

The authors would like to thank Jason Noel, Mike Daeffler, Alex Yin, Tim Noyes, Chris Flook, Kyla Smith, Jordan Beason, Jake Bonney, Connor Firmender, and Jean Carlos Blanco for their assistance in field deployments and laboratory testing. We thank Prof. Arun Shukla and Tyler Chu for their assistance with hydrostatic testing at URI. This work was supported by NSF through a Graduate Research Fellowship Award, with additional funding provided to BTP by the Office of Naval Research (Award N00014-21-1-2656). Field trials in Panamá were supported by Ocean Builders (Panamá).

Availability Statement

The dataset on which this paper is based is too large to be retained or publicly archived with available resources. Software for this research is available at the first author's github repository (https://github.com/atrunyan/stereopi_URI).

References

- Andono PN, Yuniarno EM, Hariadi M, Venus V (2012) 3D reconstruction of underwater coral reef images using low-cost multi-view cameras. ICMCS 2012. 803-808. 10.1109/ICMCS.2012.6320131.
- Armstrong RA, Pizarro O, Roman C (2019) Underwater robotic technology for imaging mesophotic coral ecosystems. Mesophotic Coral Ecosystems. 973-988.
- Bouguet JY (2004) Camera calibration tool box for matlab [eb/ol].

- Burns JHR, Fukunaga A, Pascoe KH, Runyan A, Craig BK, Talbot J, Pugh A, Kosaki RK. (2019) 3D habitat complexity of coral reefs in the Northwestern Hawaiian Islands is driven by coral assemblage structure. ISPRS-Archives. XLII-2-W10.
- Dunlop KM, Kuhn LA, Ruhl HA, Huffard CL, Caress DW, Henthorn RG, Hobson BW, McGill P, Smith Jr. KL (2015) An evaluation of deep-sea benthic megafauna length measurements obtained with laser and stereo camera methods. Deep-Sea Research I. 96: 38-48.
- Edwards CB, Eynaud Y, Williams GJ, Pedersen NE, Zgliczynski BJ, Gleason ACR, Smith JE, Sandin SA (2017) Large-area imaging reveals biologically driven non-random spatial patterns of corals at a remote reef. Coral Reefs. 36: 1291-1305.
- Ferrari R, Leon JX, Davies AJ, Burns JHR, Sandin SA, Figueira WF, Gonzalez-Rivero M (2022) Editorial: Advances in 3D habitat mapping of marine ecosystem ecology and conservation. Front. Mar. Sci. 8:827430.
- Fukunaga A, Burns JHR, Craig BK, Kosaki RK (2019) Integrating three-dimensional benthic habitat characterization techniques into ecological monitoring of coral reefs. J. Mar. Sci. Eng. 7(2), 27.
- Harvey ES & Shortis MR (1998) Calibration stability of an underwater stereo video system: implications for measurement accuracy and precision. Marine Technology Society Journal. 32(2):3-17.
- Hatcher GA, Warrick JA, Ritchie AC, Dailey ET, Zawada DG, Kranenburg C, Yates KK (2020) Accurate bathymetric maps from underwater digital imagery without ground control. Front. Mar. Sci. 7:525.
- Hirschmuller H (2008) Stereo processing by semiglobal matching and mutual information. Pattern Analysis and Machine Intelligence. IEEE Transactions on. 30(2):328–341.
- Jackson TD, Williams GJ, Walker-Springett G, Davies AJ (2020) Three-dimensional digital mapping of ecosystems: a new era in spatial ecology. Proc. R. Soc. B. 287: 20192383.
- Jackson-Bue T, Williams GJ, Walker-Springett G, Rowlands SJ, Davies AJ (2021) Three-dimensional mapping reveals scale-dependent dynamics in biogenic reef habitat structure. RSEC 7:563-699.

- Lawrence PJ, Evans AJ, Jackson-Bue T, Brooks PR, Crowe TP, Dozier AE, Jenkins SR, Moore PJ, Williams GJ, Davies AJ (2021) Artificial shorelines lack natural structural complexity across scales. *Proc. R. Soc. B.* 288:20210329.
- Leavitt G & Roman C (2018) Water quality monitoring with an autonomous surface vehicle. SURFO Technical Report No. 18-01, 15.
- Oleari F, Kallasi F, Lodi Rizzini D, Aleotti J, Caselli S (2014) Performance evaluation of a low-cost stereo vision system for underwater object detection. *IFAC World Congress* 978-3-902823-62-5/2014.
- Phillips BT, Chaloux N, Shomberg R, Muñoz-Soto A, Owens J (2021) The Fiber-Optic Reel System: A compact deployment solution for live-telemetry deep-sea robots and sensors. *Sensors* 2021, 21(7), 2526.
- Phillips BT, Licht S, Haiat KS, Bonney J, Alder J, Chalou N, Shomberg R, Noyes TJ (2019) DEEPi: A miniaturized, robust, and economical camera and computer system for deep-sea exploration. *Deep Sea Research I: Oceanographic Research Papers*. 153:103136.
- Schmidt VE & Rzhannov Y (2012) Measurement of micro-bathymetry with a GOPRO underwater stereo camera pair. 2012 Oceans, Hampton Roads, VA, USA, 2012, pp. 1-6, doi: 10.1109/OCEANS.2012.6404786.
- Shukla A, Gupta S, Matos H, LeBlanc JM (2018) Dynamic collapse of underwater metallic structures – recent investigations: contributions after the 2011 Murray Lecture. *Experimental Mechanics*. 58:387–405.
- Ubina NA, Cheng S, Chang C, Cai S, Lan H, Lu H (2022) Intelligent underwater stereo camera design for fish metric estimation using reliable object matching. *IEEE Access*. 10.1109/ACCESS.2022.3185753.
- Van Audenhaege L, Broad E, Hendry KR, Huvenne VAI (2021) High-resolution vertical habitat mapping of a deep-sea cliff offshore Greenland. *Front. Mar. Sci.* 8:669372.
- Williams K, De Robertis A, Berkowitz Z, Rooper C, Towler R (2014). An underwater stereo-camera trap. *Methods in Oceanography*. 11:1-12.
- Zhang Z (2000) A flexible new technique for camera calibration. *Pattern Analysis and Machine Intelligence. IEEE Transactions on.* 22(11):1330–1334.